Geoderma 436 (2023) 116550

Contents lists available at ScienceDirect

Geoderma

journal homepage: www.elsevier.com/locate/geoderma

Optical assessment of the spatial variation in total soil carbon using laser-induced breakdown spectroscopy

Vishal Dwivedi [a,*,1], Joni Ahokas [a,1], Jan Viljanen [a], Piotr Ryczkowski [a], Narasinha J. Shurpali [b], Hem Raj Bhattarai [b], Perttu Virkajärvi [b], Juha Toivonen [a]

[a] Photonics Laboratory, Physics Unit, Tampere University, Korkeakoulunkatu 3, 33720 Tampere, Finland
[b] Natural Resources Institute Finland, Production Systems, Grasslands and Sustainable Farming Unit, Halolantie 31 A, 71750 Maaninka, Finland

ARTICLE INFO

Handling Editor: Budiman Minasny

Keywords:
LIBS
Soil analysis
Total soil carbon
Quantification
Spatial variation

ABSTRACT

Soil carbon storage is a substantial factor in the global carbon cycle. Carbon sequestration in agricultural soils, and the assessment and validation of soil carbon storage, are crucial for the mitigation of agricultural greenhouse gas emissions and for steering towards sustainable farming practices. Enforcement and verification of carbon sequestration policies, methods, and models require extensive soil carbon monitoring capability. However, current conventional laboratory-based methods for soil carbon estimation are laborious, expensive, and time-consuming. In this work, we have developed a compact, robust, and field-capable experimental device based on laser-induced breakdown spectroscopy (LIBS) for the rapid assessment of total soil carbon content and its spatial distribution in mineral soils. The carbon content quantification was performed using a spectral line of carbon at a wavelength of 193.1 nm emitted from the laser-induced plasma plume. The LIBS measurements were performed on soil samples collected from 28 different locations and various depths (up to 1 m) of a test field cultivated with a forage legume (red clover - *Trifolium pratense*, L.) and grass (Timothy - *Phleum pratense*, L.) mixture in eastern Finland. A calibration model was established based on a limited and randomly chosen sample set and validated by comparing soil carbon estimates obtained from various locations in the test field using the dry combustion (LECO) method. Further, we demonstrate here the usefulness of LIBS methodology for mapping three-dimensional carbon distribution at the test field. We emphasize here that the calibration model can be generalized to other sample areas under similar soil type with a relative error of less than 10 % and possesses potential for fast on-site determination of spatial variation in total soil carbon, reducing substantially the need of time-consuming sample processing in laboratory. Therefore, LIBS enables frequent and extensive spatial and temporal soil carbon mapping and has the potential to become part of the future carbon monitoring network.

1. Introduction

Agriculture and associated land use changes have contributed to 24 % of all anthropogenic greenhouse gas emissions since pre-industrial times (Zomer et al., 2017), leading to global warming. Globally, soil carbon storage accounts for three times as much carbon as in the vegetation and twice the stock in the atmosphere (Smith et al., 2020). Thus, even a small change in soil carbon stock can cause significant changes in the carbon cycle. To potentially recover some of the lost soil carbon stock, implementing the best soil management practices can make soil management an effective carbon sequestration method (Lal et al., 2018). The role of soils in mitigating agricultural emissions and increasing the soil carbon storage has been emphasized in the '4 per mille' initiative, (a part of the Paris Climate Agreement signed in 2015) (Harper et al., 2018). Also, achieving the target of carbon neutral Finland 2035 requires significant emission reductions from the land use sector and strengthening carbon sinks and stocks, since carbon in Finnish agricultural soils has been declining over the past decades (Heikkinen et al., 2013; Tao et al., 2023). However, the verification and rapid monitoring of the soil carbon storage remains a major challenge (Heikkinen et al., 2021; Smith et al., 2020; Stanley et al., 2023) constraining the enforcement of policies driving soil carbon sequestration.

The current standards for soil carbon (organic or total) measurement are *ex-situ* laboratory methods. These methods are based on dry

* Corresponding author.
E-mail address: vishal.dwivedi@tuni.fi (V. Dwivedi).
[1] Contributed equally.

https://doi.org/10.1016/j.geoderma.2023.116550
Received 24 February 2023; Received in revised form 26 May 2023; Accepted 27 May 2023
Available online 2 June 2023

combustion (e.g., LECO) (Wright and Bailey, 2001), acid digestion (Maestrini and Miesel, 2017), loss on ignition (Hoogsteen et al., 2015) or in the combination of these approaches, such as Walkley-Black and Heanes methods (Conyers et al., 2011). However, *ex-situ* methods require an extensive, laborious, and time-consuming procedure for sample collection, preparation, and analyses. Also, as soil carbon is regulated by dynamic processes of carbon input and removal in a given ecosystem, it varies both spatially and temporally, thus rendering *ex-situ* lab-based methods is restrictive in assessing soil carbon storage. The labor-intensive methods lead to reduction in the number of samples that is the driving uncertainty for spatial and temporal variation in soils (Heikkinen et al., 2021; Stanley et al., 2023). The spatial and temporal variation of carbon content and its flux in soils have been tackled using flux measurements combined with computational methods (Heimsch et al., 2021; Smith et al., 2020), and the soil carbon behavior has been linked to the global climate models using Yasso soil organic carbon model (Viskari et al., 2022). However, the models are lacking extensive feedback and validation data on detailed spatial and temporal carbon behavior due to the aforementioned challenges in soil carbon monitoring.

Advanced optical spectroscopic methods enable rapid and robust investigation of soil properties (e.g., pH, organic carbon, metallic oxide contents, etc.), both remotely and *in-situ* (Gehl and Rice, 2007; Nadporozhskaya et al., 2022). Performing a soil carbon analysis in the field has the potential to reduce soil disturbance as well as enhance the ability to cover large areas than laboratory methods. For example, the methods based on the reflectance of light from soil at different wavelengths, infrared reflectometry and hyperspectral imaging, have been applied in laboratory or as remote sensing method for large areas (Chatterjee et al., 2009; Smith et al., 2020). Nonetheless, while these techniques offer certain benefits, they are also subject to limitations. Various factors, including soil moisture, color, texture, carbonate content, surface conditions, field-portability, as well as the utilization of advanced spectral libraries and data processing for accurate interpretation, pose additional challenges in meeting the requirements for cost-effective, reliable, and real-time soil carbon measurements.

A laser-based method called laser-induced breakdown spectroscopy (LIBS) has received considerable attention in various research and industrial domains for the qualitative and quantitative multi-elemental analysis of solids, liquids, and gases, covering a wide range of elements (Hahn and Omenetto, 2012; Miziolek et al., 2006). In terms of measuring soil carbon content quickly and accurately, LIBS offers a promising solution. The key advantages of LIBS over other techniques are portability, rapid analysis, no or minimal sample preparation, and the possibility of elemental mapping (Anabitarte et al., 2012; Jean-Noël et al., 2020). Also, once the appropriate spectral line is selected, LIBS analysis does not necessitate the use of any spectral libraries. In LIBS, a high-energy laser pulse is focused on the surface of the sample, causing ablation of a small volume of the material and generating a dense plasma plume. The generation of laser-induced plasma is a quasi-stationary interaction process which includes sublimation, evaporation, and extraction of particles from the materials (Giacomo and Hermann, 2017). While cooling, the plasma generates a multi-elemental emission spectrum, which is recorded and processed using statistical and mathematical approaches to obtain relevant information.

Numerous LIBS-based soil studies have produced promising outcomes. Bousquet et al. (2007), Essington et al. (2009), and Guo et al. (2019), have used LIBS for the metal and multi-elemental (Ca, Mg, Al, Fe, etc.) analysis of soil samples. Senesi and Senesi (2016), Villas-Boas et al. (2020a), and Villas-Boas et al. (2020b), have reviewed the applicability of LIBS for the elemental analysis, quantification, and classification of different soil samples and pointed out advantages and limitations for such studies. Huang et al. (2022) have reviewed the challenges and prospects of using LIBS for soil-related research. They highlight the use of various machine learning methods to address practical limitations such as matrix and self-absorption effects, feature selection, and data processing, to some extent. However, only few LIBS-based carbon studies of soils are reported in literature. Cremers et al. (2001) and Nguyen et al. (2015) demonstrated the applicability of LIBS for measuring total soil carbon in various standard and unknown soil samples, while Martin et al. (2010) have attempted a multivariate analysis for soil carbon measurements for the samples from a depth of 0–5 cm. To the best of our knowledge, no research using LIBS has been conducted on Finnish soils, which exhibits distinct characteristics due to Finland's unique environmental conditions. Furthermore, no attempt has been made to generalize calibration from a single location to another within the same field, or to fresh samples (non-sieved, non-grinded) of similar soil types from entirely different fields.

In this work, we present a compact field-capable LIBS unit and demonstrate carbon calibration model for a field block using a small set of samples from a randomly selected location of the field. The LIBS signals of the samples from a single location were calibrated against the carbon concentration obtained from LECO analysis, and the calibration curve was validated using additional 167 samples collected from the different locations and depths of the same field. The calibration model is then used to obtain spatial variation in the soil carbon content, and a complete map of carbon content variation down to the depth of 50 cm of the field is presented. Furthermore, the large-scale potential of LIBS for measuring total soil carbon is investigated on fresh soil samples collected from different agricultural fields in Finland. The carbon spectral line at a wavelength of 193.1 nm was used throughout the study.

2. Materials and methods

2.1. Study area and sample handling

In order to assess the total amount of soil carbon accurately, our sampling scheme in this study takes spatial heterogeneity of the field (uniform terrain vs. slopes) into account. We assessed total carbon from 175 mineral soil samples collected from ten different depths (0–97 cm) and 28 different locations from an 6.3 ha agricultural field, AN (63°09′49″ N, 27°14′3″ E) located in Maaninka region in eastern Finland (Fig. 1(a)) (Lind et al., 2016). Soil type of the field vary from Eutric gleysol to Luvic Planosol/Stagnosol (IUSS Working Group WRB, 2007), the topsoil (0–20 cm) being generally silt loam (mean ± standard deviation, 25.0 ± 5.6 % clay, 53.0 ± 9.0 % silt, and 22.0 ± 7.8 % sand) based on the US Department of Agriculture (USDA) textural classification system. For the same soil depth, the physiochemical characteristics (mean ± standard deviation) are: pH (H_2O) 5.8 ± 0.2, electrical conductivity 14.0 ± 2.4 $mS{\cdot}m^{-1}$, soil organic matter 5.2 ± 0.9 %, organic carbon 30.0 ± 5.2 $g{\cdot}C{\cdot}kg^{-1}$, total nitrogen 2.0 ± 0.3 $g{\cdot}N{\cdot}kg^{-1}$, C:N ratio 15.0 ± 0.4, particle density 2.7 ± 0.01 $g{\cdot}cm^{-3}$, and bulk density 1.1 ± 0.1 $g{\cdot}cm^{-3}$.

The sampling of intact soil core was done on October 19, 2020, using a tractor-mounted pneumatic drilling unit containing plastic cylinder for holding soil in intact form. The drilling unit has a maximum drilling depth of 1 m and was powered with hydraulic source. The collection of intact soil cores was done one at a time and mechanical soil compaction by tractor during the process was avoided by routing the tractor in a designated manner around the sampling locations. Additionally, the drilling was performed by keeping a minimum distance of ~2–3 m from the sampling location. All together we collected 28 intact soil cores from the entire field. Because of the natural abundance of stones in the soil, the maximum sampling depth varied between 20 and 97 cm. After collection, the plastic cylinders with intact soil cores were transported to Luke Maaninka laboratory, where they were stored at 4°C until their analyses at respective facilities, LECO at Luke Jokioinen, Finland, and LIBS at Tampere University. The plastic cores (Ø = 160 mm) were carefully opened, and the soil cores cut by knife to 10 cm intervals resulting in 175 soil samples altogether. Fig. 1(b) shows a tractor operated corer, whereas Fig. 1(c) illustrates a plastic tube used for soil

Fig. 1. (a) Map of Finland with study site AN, showing 28 sampling locations (1–28) marked with crosses, (b) tractor operated corer, (c) plastic tube used for sample collection, and (d) length-wise opened soil core.

sampling. Fig. 1(d) shows a soil core that has been lengthwise opened. Table T1 (supplementary material) summarizes the list of the samples including the GPS co-ordinates of the locations.

The carbon content of all the samples was determined using dry combustion (LECO TruMac CN, LECO Corporation, St. Joseph, Michigan, USA) in controlled and standard conditions at Luke Jokioinen, Finland. The LECO analyzer is based on the dry combustion (Dumas method) principle and is described in the literature (Wright and Bailey, 2001). Prior to LECO measurements, the samples were first oven-dried at 105°C for three hours, and then, sieved (using a 2 mm sieve) and grinded. After calibrating the LECO device using standard samples provided by manufacturers, the treated samples underwent dry combustion at high temperature inside the furnace for the evaluation of their carbon content.

2.2. LIBS experimental arrangement

LIBS has been considered as one of the most straightforward techniques for elemental monitoring from instrumentation standpoint (Rai and Thakur, 2020). Our LIBS setup is designed into a compact arrangement that can be easily transported from the lab to the field for future on-site soil measurement campaigns. The whole set-up is packed in an enclosed-box (60 cm × 45 cm × 19 cm) with a small window to place the samples. Fig. 2(a) represents the physical design of the LIBS device and Fig. 2(b) shows its internal optical scheme. A Q–switched Nd:YAG pulsed laser (LUMIBIRD Quantel, VIRON, wavelength 1064 nm, beam diameter 3.9 mm, pulse duration 8 ns) has been used to ablate a small volume of the sample and to excite a laser-induced plasma plume on the sample surface. The laser beam was guided and focused on the sample surface using a combination of optical components, i.e., Nd:YAG mirrors and a focusing lens (UV-fused silica plano-convex lens, f = 50 mm). Prior to focusing lens, a Galilean beam expander (magnifying power 4X) consisting of a C-coated bi-concave lens (f = -50 mm) as the objective lens and a C-coated plano-convex lens (f = 200 mm) as the image lens, was used to minimize the focusing spot and power density. Considering the dust produced from soil samples, optical components are mounted in such a manner that they can be removed quickly and safely for on-the-spot cleaning or replacement. Samples were placed on a motorized stage (Thorlabs) containing a customized sample holder, with the possibility of movement along the X and Y axes, while the Z-axis positioning was obtained by manually operated linear translation stage. The characteristic lifetime of laser-induced plasma, containing electrons, atoms, ions, and clusters, is in the order of several tens of microseconds (Yoon et al., 2021). The typical temperature of early plasma is in the order of ~10,000 K and when the plasma cools down, the electrons of atoms and ions in the excited electronic states fall back into their natural ground states, causing the plasma to emit radiation with discrete spectral peaks. The emission from the plasma has been collected using an optical fiber (Thorlabs BF19Y2HS02, core diameter of 200 μm), without the use of any additional collecting optics, and fed to a compact USB-connected spectrometer (Ibsen Photonics, FREEDOM UV–Vis, wavelength range 173.7 nm – 429.7 nm, resolution ~0.3 nm). The whole device is powered by battery-supplied inverter, and the major components, i.e., laser, spectrometer, and the motorized stage are connected to the PC and controlled with customized LabVIEW based interface. The specifications for the components used in the development of the LIBS device are summarized in Table 1.

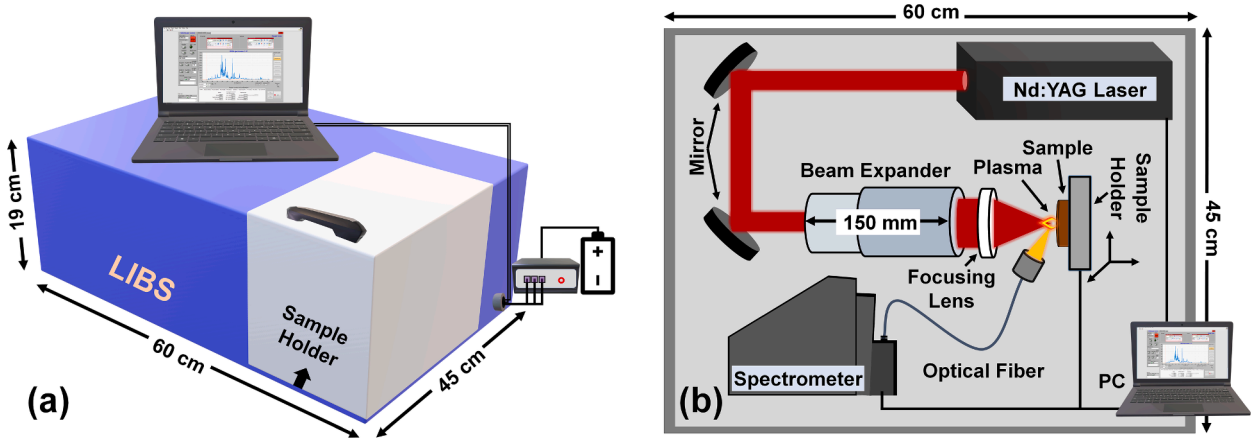

Fig. 2. (a) The physical design of the LIBS device and (b) its internal optical scheme (the components in the figure are not to scale).

Table 1
The specifications for the components used in the development of the LIBS device.

S. No.	Components	Specifications
1	Laser	LUMIBIRD Quantel, VIRON, wavelength 1064 nm, beam diameter 3.9 mm, pulse duration 8 ns, Max. Energy 51 mJ, repetition rate 1–22 Hz
2	Spectrometer	Ibsen Photonics, FREEDOM UV–Vis, wavelength range 173.7–429.7 nm, resolution ~0.3 nm
3	Translation Stage	Thorlabs (30 mm translation in X and Y) with Kinesis software, attached with a stage for manual linear translation in the Z direction
4	Mirrors	Thorlabs, Ø1″ Nd:YAG Mirror
5	Beam expander	Galilean type (magnification power 4X, length 150 mm), a combination of a Ø1″ C-coated bi-concave lens (Thorlabs, f = -50 mm) and a Ø1″ C-coated plano-convex lens (Thorlabs, f = 200 mm)
6	Focusing Lens	Thorlabs, Ø1″ UV fused silica plano-convex lens (f = 50 mm)
7	Optical Fiber	Thorlabs BF19Y2HS02, core diameter of 200 μm
8	Battery	TAB Li-Ion batteries (12.8 V, 1280 Wh) with Victron energy blue smart charger and Cotek sine wave inverter SP-1000
9	Extra	Aluminum breadboard, opto-mechanical components and screws for mounting, connecting wires and power cables
10	Software	LabVIEW (for instrument control), MATLAB (for data processing)

2.3. LIBS measurements

LIBS measurements have been performed for all the samples reported in Section 2.1 and in Table T1 (supplementary material). For LIBS measurements, the samples were pressed into circular pellets of 30 mm in diameter and of ~5 mm in thickness, using a manual bench-top press. Experimental parameters have been optimized prior to the measurements to optimize signal-to-noise ratio (SNR) for the neutral atomic spectral line of carbon at 193.1 nm. The laser pulse energy of 28 mJ was maintained throughout the measurements, while optimized acquisition time delay and exposure time were set to 600 ns and 12 μs, respectively. The repetition rate of the laser pulse was set to 5 Hz. A total of 300 spectra per sample were recorded. The sample was moved 300 μm after every laser pulse to obtain a fresh spot for a new spectrum acquisition, thus, the LIBS measurement scan area covered small portion of the pellets (15 mm × 5 mm). With these experimental settings, the measurement time is approximately one minute per sample. Table 2 presents a summary of the key experimental parameters used for the LIBS measurements.

3. Results and discussion

3.1. LIBS spectra

The spectra obtained from the individual laser shots were assorted using interquartile ranges and outlier fences to discard unsuccessful laser ablations and plasma formations leading to outliers that are typical for LIBS method. For this purpose, we divided the carbon intensity from all individual laser shots on particular sample into four quartiles, with boundaries Q0-Q1, Q1-Q2, Q2-Q3, and Q3-Q4. The outlier exclusion limits are then adjusted to include data points in the second, third, and fourth quartiles (only two-thirds of the data points from the fourth quartile having intensities within the standard deviation limit of the third quartile were included). After removing outliers using aforementioned statistical approach, it was found that the remaining about 200 spectra from the original 300 individual spectra are within the range of mean ± 2 × standard deviation (σ), which also shows the stability of our LIBS measurements in terms of laser shot-to-shot variation (Lazic et al., 2005). Fig. 3 shows an example of the statistical distribution of carbon spectral line intensity of 200 spectra from location A12 at a depth of 40–50 cm, which were ultimately considered for further analysis. The relative standard deviation (RSD) of these 200 spectral data points was determined to be 4.3 %. In order to compare this variation in soil samples with a homogeneous matrix, we conducted a supplementary exercise by measuring pure copper sample under the same experimental settings, and the RSD for the shot-to-shot intensity variation of the Cu spectral line at 324.8 nm was calculated to be 2.9 %, from 200 spectra. This difference can be attributed to the small-scale spatial variability on soil sample. All other soil samples have also shown a similar variation. Furthermore, the repeatability of the measurements was tested by measuring the same soil sample fifteen times and the uncertainty in the LIBS carbon intensity was found to be approximately ± 3 %. Averaging over hundreds of spectra collected from different points of the sample mitigates the problem of shot-to-shot variation in spectral data and inhomogeneity of the samples (Chen et al., 2018).

In LIBS applications, carbon is often detected using the emission line at 247.8 nm (Cremers et al., 2001). However, the current research is performed using soil samples from a Finnish agriculture site that is iron rich and the emission by iron atoms interferes with this carbon line. For this reason, we made the decision to extend our detection range to the deep-UV part of the spectrum and to use the carbon spectral line at 193.1 nm instead. Fig. 4(a) shows an example of the variation of the carbon spectral line intensity and shape at different depths, for sample set from the location A12. The only possibility of interfering 193.1 nm carbon spectral line is Al ionic spectral line, that is evident from the right bump in the raw data shown in Fig. 4(a). Fig. 4(b) shows an example of the fitting of carbon spectral line at 193.1 nm and its deconvolution from the neighboring Al (ionic) spectral line at 193.5 nm from the top layer (0–10 cm) of the sample set from location A12. In order to evaluate the area under the carbon spectral line, the spectral lines were fitted with the Pseudo-Voigt profile (Dwivedi et al., 2021; Marín Roldán et al., 2021). Spectral lines have been identified using NIST atomic spectral database (Kramida et al., 2022). The very same strategy has been used for the analysis of all the examined samples. In Fig. 4(a) and Fig. 4(b), a

Table 2
Summary of the key experimental parameters used for the LIBS measurements.

S. No.	Experimental parameters	Value
1	Laser pulse energy	28 mJ
2	Laser repetition rate	5 Hz
3	Laser pulse duration	8 ns
4	Acquisition delay time	600 ns
5	Acquisition exposure time	12 μs
6	No. of spectra per sample	300

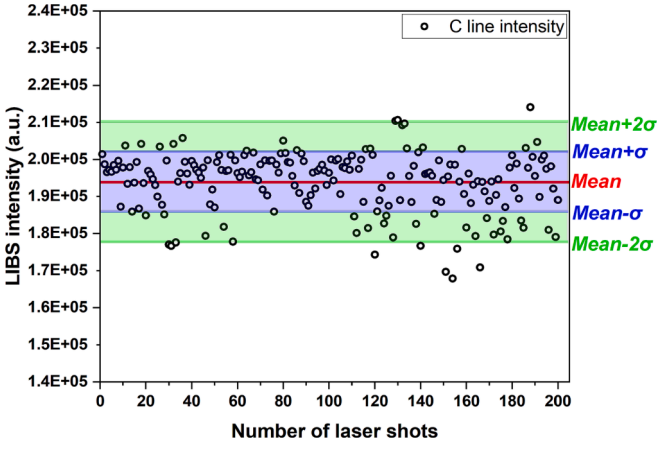

Fig. 3. An example of laser shot-to-shot variation for carbon line intensity for the sample from A12 location at the depth of 40–50 cm. Horizontal lines for mean value, mean ± σ, and mean ± 2σ are also shown.

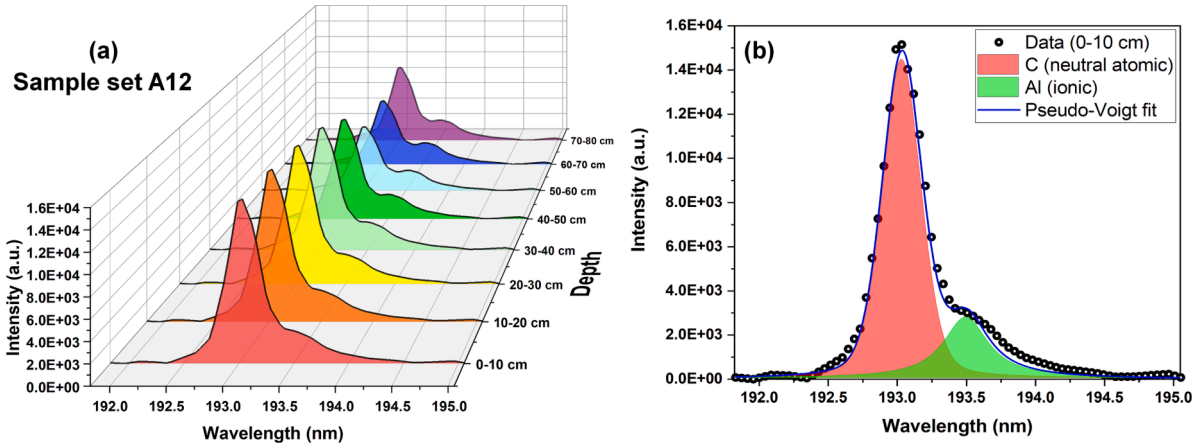

Fig. 4. (a) An example of variation of the carbon spectral line at 193.1 nm with depth (cm) for sample set from the location A12 and (b) fitting of the spectral lines present within the spectral range from 192 nm to 195 nm for the sample from the top layer (0–10 cm) of location A12. In both figures, the y-axis represents the intensity of the spectral lines in arbitrary units.

higher integrated intensity of the spectral line indicates a higher content of carbon.

3.2. Calibration plot

The LIBS signal intensities of the carbon line from the small sample set (eight samples) of a single location A12, that is randomly chosen from the central part of the field, were calibrated using the carbon concentration values obtained from LECO measurements. The choice of location also requires considering the wide range of carbon content that is 2–65 g·kg^{-1} for the samples from location A12. Considering the direct relationship between both quantities (LIBS signal intensity and LECO carbon concentration), a simple univariate regression has been used for the calibration. Fig. 5 shows the calibration curve using logarithmic fitting and includes a 95 % confidence interval. The calibration curve shows a non-linear trend with a high coefficient of determination, R^2 value of 0.98. It has been observed that the sensitivity decreases with increasing carbon content, that is due to the increasing self-absorption of the radiation by the atomic carbon in the plasma plume (Lazic et al., 2001). While the self-absorption effect can be significant for the elements with strong spectral lines and high concentrations in the sample, it was not a major concern in our study as the majority of samples had a carbon content less than 50 (g·kg^{-1}).

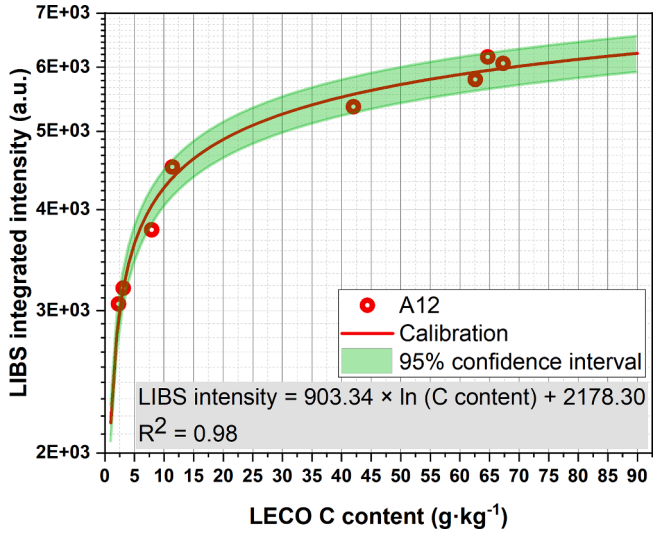

Fig. 5. Calibration plot for the sample set from different depths at location A12 using LIBS carbon line intensity and carbon content (g·kg^{-1}) obtained from LECO measurements. The 95 % confidence interval has also been included in the figure. LIBS intensity axis is plotted using logarithmic scale for better visualization.

3.3. Validation of LIBS results: Comparison with LECO

All samples investigated with LIBS were also analyzed using the LECO method in order to gain a better understanding of the uncertainties in the LIBS results. Among the 175 samples collected from different locations and depths of the field, only a small set of eight samples (from location A12) were used to construct calibration curve, while the calibration curve was validated by the additional 167 samples. Fig. 6 shows a calibration curve along with LIBS validation data and confidence intervals of 90 % and 95 %. Even though there are variations in the soil type and properties, i.e., in the soil matrix within the test field (see Table T1, supplementary material) and the soil itself is complex in nature, all the data points follow the same trend as obtained from a single randomly chosen location (A12). Based on a thorough examination of Fig. 6, with the exception of a few data points, all validation points fall within the 90 % confidence interval. The data points that are outside the confidence interval are mainly from locations that are

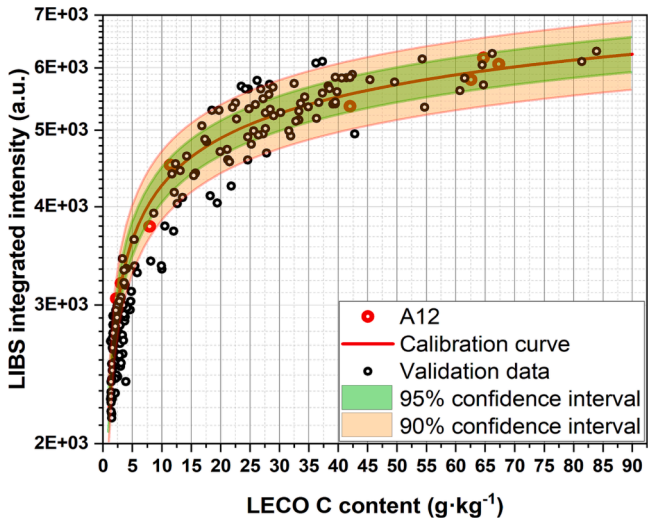

Fig. 6. Calibration curve and confidence intervals (90 % and 95 %) for sample set from the location A12 and validation data points from the additional 167 samples.

slightly different in terms of soil type from the ones used for the construction of the calibration curve (see Table T1 for details). Furthermore, the variation in the validation data points in Fig. 6 is also due to soil matrix differences, soil properties, e.g., structure and morphology, and the inaccuracy of LECO measurements (Wright and Bailey, 2001). Thus, a calibration model constructed from a single location's sample set can be used to obtain the carbon content of any random sample of a similar soil type with an uncertainty of less than ± 10 %.

3.4. Spatial variation of carbon content

To demonstrate the ability to assess spatial variation in the carbon content for the test field, samples from various locations (A1-A28) and depths down to 1 m at 10 cm intervals were analyzed using LIBS. The specifics of these locations are provided as Table T1 (supplementary material). Fig. 7 shows an example of carbon content depth variation obtained from LIBS measurements at five locations: A16, A17, A18, A20 and A27. For A18 and A20, soil sampling was done to a depth of 97 cm and 80 cm, respectively, whereas for other locations (A16, A17, and A27), soil samples were collected from up to a depth of 90 cm (see Table T1, supplementary material). It is observed that the LIBS carbon emission line intensity and, subsequently, the carbon depth distribution obtained with the calibration presented in Section 3.2 follow the expected soil carbon distribution trend (Balesdent et al., 2018; Sulman et al., 2020). The samples in the top three layers (0–10 cm, 10–20 cm, and 20–30 cm) have significantly higher carbon content than those in the other layers after 30 cm depth. This is due to the organic carbon originating from vegetation, e.g., from roots and crop litter, and remains mainly in the uppermost soil layer, i.e., in depth of 0–30 cm. It should also be noted that the carbon content is not necessarily the same at different locations within the layer, highlighting the ability of LIBS to detect variability across various positions within the field. (Heikkinen et al., 2021; Lind et al., 2016). Moreover, at some locations, e.g., at A16, a slight increase in carbon signal was observed after 60 cm or 70 cm depth.

Fig. 8(a) depicts the spatial pattern of carbon content in the top layer (0–10 cm) of the investigated field as determined by LIBS measurements. The cubic spline interpolation method has been used to obtain the complete carbon map. The associated uncertainty level of the measurement points on the map varies from ± 5 to ± 10 %, varying from site to site. The precision of the map and the interpolation across the field depend on the sampling density and can be further improved. However,

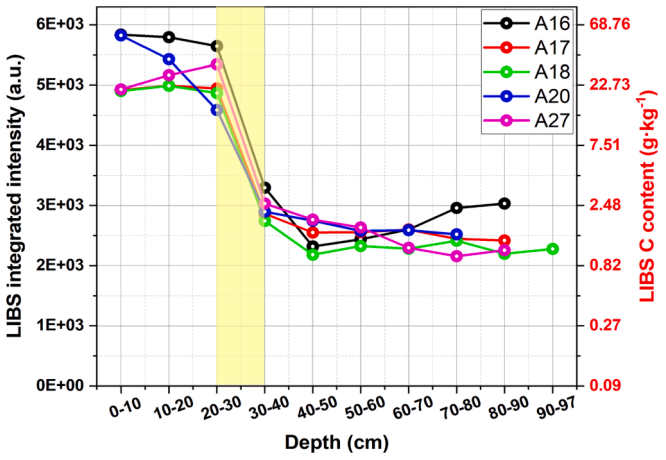

Fig. 7. An example of carbon content variation obtained from LIBS measurements at five sites: A16, A17, A18, A20 and A27. The y-axis at right side of the figure is showing carbon content (g·kg^{-1}) evaluated using calibration curve (Fig. 5). The yellow highlighted portion is showing the transition of carbon content below 30 cm in depth. (For interpretation of the references to color in this figure legend, the reader is referred to the web version of this article.)

the aim of presenting such a map is to demonstrate the capabilities of the LIBS technique. It is interesting to note that within the same layer, there is a significant variation in carbon concentrations, which is reflected in LIBS carbon signal levels. From Fig. 8(a), it can be observed that locations A12, A15, A16, and A22 have higher carbon concentration than the other locations, while locations A25 and A26 have relatively lower carbon concentration. Combining the spatial distribution of carbon content for the layers from different depths results in a complete map of the spatial carbon distribution throughout the entire test field. The Fig. 8 (b) illustrates the complete measured and interpolated carbon distribution for first five layers of the field (0–50 cm). The corresponding carbon content values reported in Fig. 8 have been estimated using calibration curve presented in Fig. 5.

3.5. Robustness of the calibration model

To test the robustness and generality of the calibration model, LIBS measurements were performed on fifteen, non-grinded and non-sieved samples from two fields that are located in different region in southern Finland than the test field used for calibration and validation. Six samples are from the KO field and nine samples are from the LA field (Mattila and Girz, 2021). Both fields are classified as silty loam and their carbon content ranges in 2–20 g·kg^{-1}. After collection from the field in 2021, the samples were stored and then dried, pelletized, and measured with LIBS method in accordance with the procedure described in Sections 2.2 and 2.3 and using LECO specified in Section 2.1.

The LIBS carbon emission intensities obtained from new locations are compared to the calibration models fitted to the old location single core A12 data set and to the calibration curve obtained from fit to all A1-28 data sets. The fitted calibration curves are different as the A1-A28 curve contains also the data points from all soil types that were present in the AN field data set. Both calibration curves are shown in Fig. 9 together with confidence intervals of 90 % and 95 % for the A1-A28 curve, along with individual points depicting that the LIBS measurements of the samples from KO and LA field follow the calibration model from AN field, despite the differences in the sample processing, field locations, and subsequent differences in the soil matrixes. All KO and LA data points are within the 90 % confidence interval of the calibration model fitted to A1–28 data set, thus demonstrating that a robust and general calibration model can be formed with an uncertainty of less than ± 10 %, to determine total soil carbon spatial variation in a field volume.

The results presented in Fig. 9 highlight that the spatial distribution of the total soil carbon content in an agricultural field can be obtained on-site (with an uncertainty of less than ± 10 %) using prior calibration with similar soil type. The carbon analysis process performed in this section for sample preparation (sample pelletization and drying) and the LIBS analysis itself that can be performed onsite within a few minutes, allowing a spatial distribution map of the total soil carbon content to be obtained rapidly. The obtained distribution map provides feedback on how many samples need to be processed and analyzed further to obtain reliable carbon estimation, thus resolving a concern that has been recently raised as one of the main problems in soil carbon models (Stanley et al. 2023). In addition, if more accurate calibration is desired for the LIBS measurement, a calibration curve from around ten samples with a wide range of carbon content is sufficient to provide improved calibration for the sample set at hand. To generalize the calibration model and compare it to current mainstream modeling approaches for substantially varying soil types requires future work.

The LIBS is an information rich method, and it has the ability to analyze multiple elements simultaneously, depending on the spectrograph's range. However, selecting an appropriate spectral line is a key factor in the LIBS analysis. In this study, we have focused solely on carbon content analysis. The typical spectral line for carbon in LIBS analysis is 247.8 nm, but due to the interference with iron spectral line from iron-rich Finnish soil, we have designed our set-up which is capable of detecting 193.1 nm spectral line. Although this line also partially

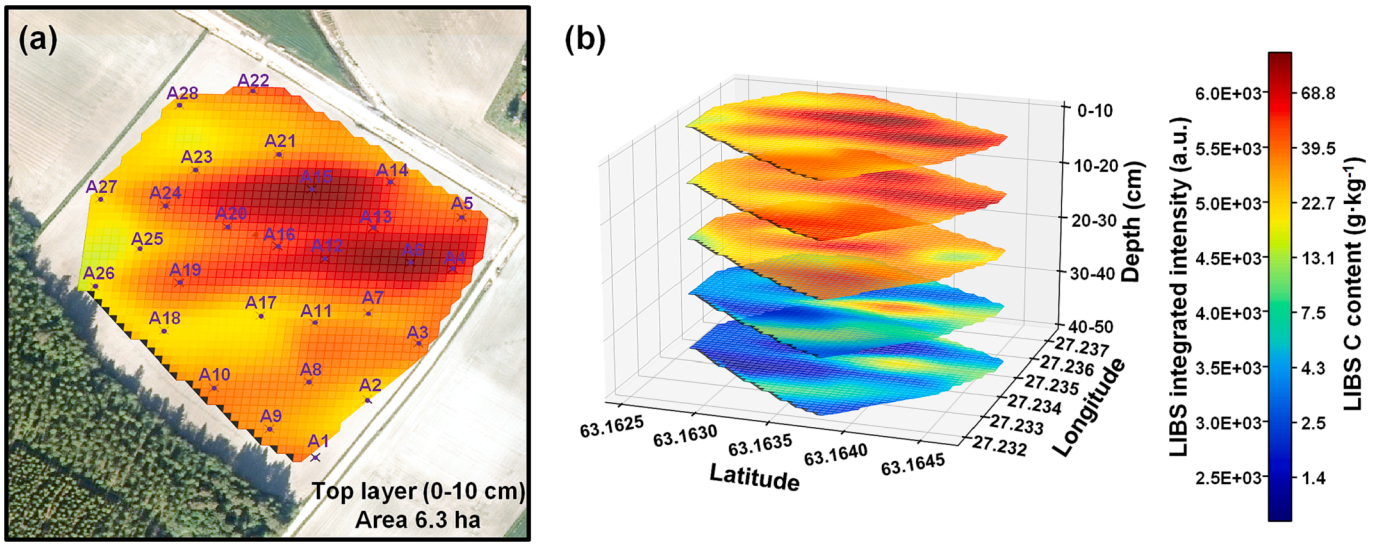

Fig. 8. (a) Spatial pattern of total soil carbon within the top layer (0–10 cm) and (b) 3D map of carbon for five layers (0–50 cm) of the AN test field obtained using LIBS method. The carbon content (g·kg^{-1}) included in color-bar are evaluated using calibration curve in Fig. 5.

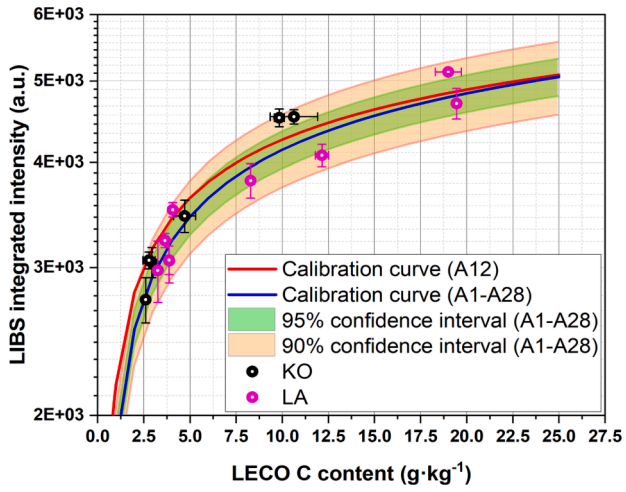

Fig. 9. The calibration curve from one single location (A12), calibration curve from all locations (A1-A28) of the AN field, confidence intervals of 90 % and 95 % for the calibration curve from all locations, and measurements of the samples from KO and LA fields. Statistical error bars for both x- and y- axes have also been included for the data points from KO and LA.

overlaps with the ionic spectral line of aluminum, we used a spectral line fitting and deconvolution approach to extract the carbon intensity from the observed envelope. Furthermore, the LIBS spectral information can be utilized to identify the soil type using multivariate calibration methods and/or machine learning to place the obtained carbon signal to a correct calibration curve. LIBS also possesses the potential for identification of micro variations in the soil composition. The LIBS spot size is in the order of hundreds of micrometers thus, the spectral shot-to-shot variation can be used to distinguish mineral and organic granules in, e.g., sandy forest soils that have large variation in particle size.

Taking into account the possible limitations of our work, it is important to note that while LIBS technology can provide valuable information on total soil carbon content, it is challenging to predict the presence of inorganic carbon from the spectral data. Also, the accuracy of the carbon map can be improved by increasing the number of sampling points, but this also increases the time and effort required for soil sample collection. This is a key concern addressed in our work. Our work was designed to keep a perfect balance between precision and practicality by considering the involved trade-offs.

4. Conclusions

In the realm of soil research and analysis, LIBS technique is emerging and has the benefit due to its simplicity, rapidity, and cost-effectiveness. In this study, we have developed a compact and robust LIBS device that can be easily transported to the fields for on-site soil analysis. Further, we have presented a calibration model for quantification of total soil carbon that is based on a small set of samples from a randomly selected location of the field and validated using additional 167 samples (with carbon content ranging from 1 to 85 g·kg^{-1}) from the different locations of the same field. The obtained calibration model is then applied to demonstrate measurement of 3D spatial variation of total soil carbon in the test field. From the spatial variation of carbon content over the examined field, significant inter- and intra-layer variation in the LIBS intensity of carbon and, thus, in the carbon concentration, was observed. Additionally, it was observed that the LIBS intensity variation is nearly linear for samples with a low carbon content (less than 5 g·kg^{-1}); however, with increasing carbon content, the sensitivity decreases due to the increasing self-absorption of the radiation by the atomic species in the plasma plume. The robustness of the calibration model was demonstrated by comparing the LIBS method calibration to fresh and unprocessed samples from two different fields of similar soil type but from different geographical locations as the field used for calibration. The global relative uncertainty in LIBS results was found to be about ± 10 %, which may be attributed to soil matrix differences, soil properties, e.g., types, structure, and morphology, and the inaccuracy of LECO measurements in addition to normal statistical variation from LIBS. In comparison to LECO analysis, the LIBS analysis is simple and fast, with measurement time of only about one minute per sample. In addition, LIBS analysis can be performed on-site reducing the need of soil storage capacity and, as the calibration for a field block can be obtained from a small number of samples, the sample handling in laboratory is reduced substantially. Hence, LIBS enables spatial and temporal frequent carbon monitoring without extensive laboratory work and has the potential to become part of the future carbon monitoring network.

CRediT authorship contribution statement

Vishal Dwivedi: Methodology, Formal analysis, Data curation, Investigation, Software, Visualization, Writing – original draft. **Joni**

Ahokas: Methodology, Formal analysis, Visualization, Investigation, Writing – review & editing. **Jan Viljanen:** Conceptualization, Writing – review & editing, Funding acquisition. **Piotr Ryczkowski:** Methodology, Software. **Narasinha J. Shurpali:** Resources, Writing – review & editing. **Hem Raj Bhattarai:** Writing – review & editing. **Perttu Virkajärvi:** Resources, Supervision, Writing – review & editing, Funding acquisition. **Juha Toivonen:** Conceptualization, Resources, Supervision, Writing – review & editing, Funding acquisition.

Declaration of Competing Interest

The authors declare that they have no known competing financial interests or personal relationships that could have appeared to influence the work reported in this paper.

Data availability

Data will be made available on request.

Acknowledgments

The authors are grateful for the collaboration over the Carbon Action platform. This work was supported by the Academy of Finland Flagship Programme PREIN (grant 320165) and the Ministry of Agriculture and Forestry of Finland (decisions VN/5275/2021). J.V. and N.J.S. acknowledge funding from the Academy of Finland (decisions: 338338 and 334422). P.V. and N.J.S. also acknowledge funding from the Ministry of Agriculture and Forestry of Finland, ORMINURMI, ORMINURMI 2, and NC-GRASS (VN/28562/2020-MMM-2).

Appendix A. Supplementary data

Supplementary data to this article can be found online at https://doi.org/10.1016/j.geoderma.2023.116550.

References

Anabitarte, F., Cobo, A., Lopez-Higuera, J.M., 2012. Laser-induced breakdown spectroscopy: fundamentals, applications, and challenges. Internat. Schol. Res. Notices. https://doi.org/10.5402/2012/285240 e285240.

Balesdent, J., Basile-Doelsch, I., Chadoeuf, J., Cornu, S., Derrien, D., Fekiacova, Z., Hatté, C., 2018. Atmosphere–soil carbon transfer as a function of soil depth. Nature 559, 599–602. https://doi.org/10.1038/s41586-018-0328-3.

Bousquet, B., Sirven, J.-B., Canioni, L., 2007. Towards quantitative laser-induced breakdown spectroscopy analysis of soil samples. Spectrochim. Acta Part B: Atomic Spectrosc. 62 (12), 1582–1589.

Chatterjee, A., Lal, R., Wielopolski, L., Martin, M.Z., Ebinger, M.H., 2009. Evaluation of different soil carbon determination methods. Crit. Rev. Plant Sci. 28, 164–178. https://doi.org/10.1080/07352680902776556.

Chen, C.P., Hei, L., Yu, S.C., Chen, W.L., Cai, M.X., 2018. Application of laser induced breakdown spectroscopy in soil element analysis of watershed. MATEC Web Conf. 246, 01114. https://doi.org/10.1051/matecconf/201824601114.

Conyers, M.K., Poile, G.J., Oates, A.A., Waters, D., Chan, K.Y., Conyers, M.K., Poile, G.J., Oates, A.A., Waters, D., Chan, K.Y., 2011. Comparison of three carbon determination methods on naturally occurring substrates and the implication for the quantification of 'soil carbon'. Soil Res. 49, 27–33. https://doi.org/10.1071/SR10103.

Cremers, D.A., Ebinger, M.H., Breshears, D.D., Unkefer, P.J., Kammerdiener, S.A., Ferris, M.J., Catlett, K.M., Brown, J.R., 2001. Measuring total soil carbon with laser-induced breakdown spectroscopy (LIBS). J. Environ. Quality 30, 2202–2206. https://doi.org/10.2134/jeq2001.2202.

De Giacomo, A., Hermann, J., 2017. Laser-induced plasma emission: from atomic to molecular spectra. J. Phys. D: Appl. Phys. 50 (18), 183002.

Dwivedi, V., Marín-Roldán, A., Karhunen, J., Paris, P., Jõgi, I., Porosnicu, C., Lungu, C.P., van der Meiden, H., Hakola, A., Veis, P., 2021. CF-LIBS quantification and depth profile analysis of Be coating mixed layers. Nucl. Mater. Energy 27, 100990. https://doi.org/10.1016/j.nme.2021.100990.

Essington, M.E., Melnichenko, G.V., Stewart, M.A., Hull, R.A., 2009. Soil metals analysis using laser-induced breakdown spectroscopy (LIBS). Soil Sci. Soc. Am. J. 73, 1469–1478. https://doi.org/10.2136/sssaj2008.0267.

Gehl, R.J., Rice, C.W., 2007. Emerging technologies for in situ measurement of soil carbon. Clim. Change 80, 43–54. https://doi.org/10.1007/s10584-006-9150-2.

Guo, G., Niu, G., Shi, Q., Lin, Q., Tian, D., Duan, Y., 2019. Multi-element quantitative analysis of soils by laser induced breakdown spectroscopy (LIBS) coupled with univariate and multivariate regression methods. Anal. Methods 11, 3006–3013. https://doi.org/10.1039/C9AY00890J.

Hahn, D.W., Omenetto, N., 2012. Laser-induced breakdown spectroscopy (LIBS), part II: review of instrumental and methodological approaches to material analysis and applications to different fields. Appl. Spectrosc. 66, 347–419. https://doi.org/10.1366/11-06574.

Harper, A.B., Powell, T., Cox, P.M., House, J., Huntingford, C., Lenton, T.M., Sitch, S., Burke, E., Chadburn, S.E., Collins, W.J., Comyn-Platt, E., Daioglou, V., Doelman, J. C., Hayman, G., Robertson, E., van Vuuren, D., Wiltshire, A., Webber, C.P., Bastos, A., Boysen, L., Ciais, P., Devaraju, N., Jain, A.K., Krause, A., Poulter, B., Shu, S., 2018. Land-use emissions play a critical role in land-based mitigation for Paris climate targets. Nat Commun 9, 2938. https://doi.org/10.1038/s41467-018-05340-z.

Heikkinen, J., Ketoja, E., Nuutinen, V., Regina, K., 2013. Declining trend of carbon in Finnish cropland soils in 1974–2009. Global Change Biol. 19, 1456–1469. https://doi.org/10.1111/gcb.12137.

Heikkinen, J., Keskinen, R., Regina, K., Honkanen, H., Nuutinen, V., 2021. Estimation of carbon stocks in boreal cropland soils - methodological considerations. Eur. J. Soil Sci. 72, 934–945. https://doi.org/10.1111/ejss.13033.

Heimsch, L., Lohila, A., Tuovinen, J.-P., Vekuri, H., Heinonsalo, J., Nevalainen, O., Korkiakoski, M., Liski, J., Laurila, T., Kulmala, L., 2021. Carbon dioxide fluxes and carbon balance of an agricultural grassland in southern Finland. Biogeosciences 18, 3467–3483. https://doi.org/10.5194/bg-18-3467-2021.

Hoogsteen, M.J.J., Lantinga, E.A., Bakker, E.J., Groot, J.C.J., Tittonell, P.A., 2015. Estimating soil organic carbon through loss on ignition: effects of ignition conditions and structural water loss. Eur. J. Soil Sci. 66, 320–328. https://doi.org/10.1111/ejss.12224.

Huang, Y., Harilal, S.S., Bais, A., Hussein, A.E., 2022. Progress toward machine learning methodologies for laser-induced breakdown spectroscopy with an emphasis on soil analysis. IEEE Trans. Plasma Sci. 1–21 https://doi.org/10.1109/TPS.2022.3231985.

Jean-Noël, M.K., Arthurb, K.T., Jean-Marcc, B., 2020. LIBS technology and its application: overview of the different research areas. J. Environ. Sci. Public Health 4, 134–149. https://doi.org/10.26502/jesph.96120090.

Kramida, A., Ralchenko, Y., Reader, J., NIST ASD Team, 2022. Atomic Spectra Database. NIST.

Lal, R., Smith, P., Jungkunst, H.F., Mitsch, W.J., Lehmann, J., Nair, P.K.R., McBratney, A. B., de Moraes Sá, J.C., Schneider, J., Zinn, Y.L., Skorupa, A.L.A., Zhang, H.-L., Minasny, B., Srinivasrao, C., Ravindranath, N.H., 2018. The carbon sequestration potential of terrestrial ecosystems. J. Soil Water Conserv. 73, 145A–152A. https://doi.org/10.2489/jswc.73.6.145A.

Lazic, V., Barbini, R., Colao, F., Fantoni, R., Palucci, A., 2001. Self-absorption model in quantitative laser induced breakdown spectroscopy measurements on soils and sediments. Spectrochim. Acta B At. Spectrosc. 56 (6), 807–820.

Lazic, V., Colao, F., Fantoni, R., Spizzicchino, V., 2005. Laser-induced breakdown spectroscopy in water: Improvement of the detection threshold by signal processing. Spectrochim. Acta B At. Spectrosc. 60 (7-8), 1002–1013.

Lind, S.E., Shurpali, N.J., Peltola, O., Mammarella, I., Hyvönen, N., Maljanen, M., Räty, M., Virkajärvi, P., Martikainen, P.J., 2016. Carbon dioxide exchange of a perennial bioenergy crop cultivation on a mineral soil. Biogeosciences 13, 1255–1268. https://doi.org/10.5194/bg-13-1255-2016.

Maestrini, B., Miesel, J.R., 2017. Modification of the weak nitric acid digestion method for the quantification of black carbon in organic matrices. Org Geochem. 103, 136–139. https://doi.org/10.1016/j.orggeochem.2016.10.010.

Martin, M.Z., Labbé, N., André, N., Wullschleger, S.D., Harris, R.D., Ebinger, M.H., 2010. Novel multivariate analysis for soil carbon measurements using laser-induced breakdown spectroscopy. Soil Sci. Soc. Am. J. 74, 87–93. https://doi.org/10.2136/sssaj2009.0102.

Mattila, T., Girz, A., 2021. Carbon action MULTA Finnish carbon sequestration experimental field dataset 2021. https://doi.org/10.5281/zenodo.5575531.

Miziolek, A.W., Palleschi, V., Schecter, I., 2006. Laser Induced Breakdown Spectroscopy. Cambridge University Press.

Nadporozhskaya, M., Kovsh, N., Paolesse, R., Lvova, L., 2022. Recent advances in chemical sensors for soil analysis: A review. Chemosensors 10, 35. https://doi.org/10.3390/chemosensors10010035.

Nguyen, H.-V.-M., Moon, S.-J., Choi, J.H., 2015. Improving the application of laser-induced breakdown spectroscopy for the determination of total carbon in soils. Environ. Monit. Assess 187, 28. https://doi.org/10.1007/s10661-015-4286-z.

Rai, V.N., Thakur, S.N., 2020. Chapter 5 - Instrumentation for LIBS and recent advances. In: Singh, J.P., Thakur, S.N. (Eds.), Laser-Induced Breakdown Spectroscopy, second ed. Elsevier, Amsterdam, pp. 107–136. 10.1016/B978-0-12-818829-3.00005-8.

Roldán, A.M., Dwivedi, V., Veis, M., Atikukke, S., van der Meiden, H., Držík, M., Veis, P., 2021. Quantification of hydrogen isotopes by CF-LIBS in a W-based material (WZr) at atmospheric pressure: from ns towards ps. Phys. Scr. 96 (12), 124061.

Senesi, G.S., Senesi, N., 2016. Laser-induced breakdown spectroscopy (LIBS) to measure quantitatively soil carbon with emphasis on soil organic carbon. A review. Anal. Chim. Acta 938, 7–17. https://doi.org/10.1016/j.aca.2016.07.039.

Smith, P., Soussana, J., Angers, D., Schipper, L., Chenu, C., Rasse, D.P., Batjes, N.H., Egmond, F., McNeill, S., Kuhnert, M., Arias-Navarro, C., Olesen, J.E., Chirinda, N., Fornara, D., Wollenberg, E., Álvaro-Fuentes, J., Sanz-Cobena, A., Klumpp, K., 2020. How to measure, report and verify soil carbon change to realize the potential of soil carbon sequestration for atmospheric greenhouse gas removal. Glob. Chang. Biol. 26, 219–241. https://doi.org/10.1111/gcb.14815.

Stanley, P., Spertus, J., Chiartas, J., Stark, P.B., Bowles, T., 2023. Valid inferences about soil carbon in heterogeneous landscapes. Geoderma 430, 116323. https://doi.org/10.1016/j.geoderma.2022.116323.

Sulman, B.N., Harden, J., He, Y., Treat, C., Koven, C., Mishra, U., O'Donnell, J.A., Nave, L.E., 2020. land use and land cover affect the depth distribution of soil carbon:

insights from a large database of soil profiles. Front. Environ. Sci. 8, 146. https://doi.org/10.3389/fenvs.2020.00146.

Tao, F., Palosuo, T., Lehtonen, A., Heikkinen, J., Mäkipää, R., 2023. Soil organic carbon sequestration potential for croplands in Finland over 2021–2040 under the interactive impacts of climate change and agricultural management. Agr. Syst. 209, 103671 https://doi.org/10.1016/j.agsy.2023.103671.

Villas-Boas, P.R., Franco, M.A., Martin-Neto, L., Gollany, H.T., Milori, D.M.B.P., 2020a. Applications of laser-induced breakdown spectroscopy for soil analysis, part I: Review of fundamentals and chemical and physical properties. Eur. J. Soil Sci. 71, 789–804. https://doi.org/10.1111/ejss.12888.

Villas-Boas, P.R., Franco, M.A., Martin-Neto, L., Gollany, H.T., Milori, D.M.B.P., 2020b. Applications of laser-induced breakdown spectroscopy for soil characterization, part II: Review of elemental analysis and soil classification. Eur. J. Soil Sci. 71, 805–818. https://doi.org/10.1111/ejss.12889.

Viskari, T., Pusa, J., Fer, I., Repo, A., Vira, J., Liski, J., 2022. Calibrating the soil organic carbon model Yasso20 with multiple datasets. Geosci. Model Dev. 15, 1735–1752. https://doi.org/10.5194/gmd-15-1735-2022.

Wright, A.F., Bailey, J.S., 2001. Organic carbon, total carbon, and total nitrogen determinations in soils of variable calcium carbonate contents using a Leco CN-2000 dry combustion analyzer. Commun. Soil Sci. Plant Anal. 32, 3243–3258. https://doi.org/10.1081/CSS-120001118.

Yoon, S., Choi, H.-W., Kim, J., 2021. Analysis of changes in spectral signal according to gas flow rate in laser-induced breakdown spectroscopy. Appl. Sci. 11, 9046. https://doi.org/10.3390/app11199046.

Zomer, R.J., Bossio, D.A., Sommer, R., Verchot, L.V., 2017. Global sequestration potential of increased organic carbon in cropland soils. Sci. Rep. 7, 15554. https://doi.org/10.1038/s41598-017-15794-8.